Fluidization and Fluid Particle Systems: Recent Advances

George E. Klinzing, editor

1984

Fluidization and Fluid Particle Systems: Recent Advances

George E. Klinzing, editor

Ismail Alkan
M.A. Bergougnou
J.D. Bingle
Jacques Bouillard
M. Butensky
H.S. Caram
J.C. Cassulo
I.H. Chan
T.K. Chen
Y.O. Chong
J.K. Claflin
Manuk Colakyan
C.A. Coulaloglou
H.I. de Lasa
Bozorg Ettediah
Liang-Shih Fan
A.G. Fane
D. Fountain
K. Fujie
J.D. Gabor
Dimitri Gidaspou
S. Hiraoka
Tho-Ching Ho
J.R. Hopper
D.G. Horne
D. Hyman
M. Jinnai
Mitsou Kamiwano
Hugo Karam
George E. Klinzing
T.M. Knowlton
Hisashi O. Kono
Milton B. Larson
S.L.P. Lee
L.S. Leung
Octave Levenspiel
Edward K. Levy
T.R. Long
Mahendra P. Mathur
Q.M. Mao
S. Miho
S. Mori
Thu-Hang Nguyen
Fan Ouyang
B. Patrose
O.E. Potter
G.J. Quarderer
P.N. Rowe
Fumio Saito
J.H. Seigell
M. Shao
V.T. Sinha
Chi Tien
C.S. Teo
S.T. Tuba
K. Ushiki
L. Wasserzug
A.W. Weimer
H. Weinstein
D.J. Wildman
Y. Xiao-tian
I. Yamada
J.G. Yates
Guo-Tai Zhang

AIChE shall not be responsible for statements or opinions advanced in papers or printed in its publications.

Library of Congress Cataloging in Publication Data
Main entry under title:

Fluidization and fluid particle systems.

(AIChE symposium series ; v. 80, no. 241)
"A selected group of papers presented at the 76th Annual Meeting of the American Institute of Chemical Engineers at San Francisco in November of 1984"—
1. Fluidization—Congresses. I. Klinzing, George E. II. American Institute of Chemical Engineers. Meeting (76th : 1984 : San Francisco, Calif.) III. Series : AIChE symposium series ; no. 241.
TP156.F65F5735 1985 660.2'842 85-7558
ISBN 0-8169-0335-2

Printed in the United States of America by Twin Production & Design

FOREWORD

This present volume on fluidization and fluid-particle systems is a result of a selected group of papers presented at the 76th Annual Meeting of the American Institute of Chemical Engineers at San Francisco in November of 1984. At this meeting four sessions on the topic covered both fundamental and applied contributions in addition to a session on heat transfer in fluidization.

Solids handling by fluidization technology and fluid-particle system continues to be prevalent in industry and the research laboratory. Many new findings and novel applicatons are surfacing each year. This present volume represents a composite summary of this fast changing field.

The contents can be roughly characterized by contributions to modeling internal bubble behavior and distributors and disengaging sections of fluidization beds. In addition, heat transfer, three phase beds, magnetic beds and inclined beds are presented. Filtration and pneumatic transport topics are contributions to the fluid-particle systems area.

George E. Klinzing, *editor*
Carnegie-Mellon University
Pittsburgh, PA 15213

SYMPOSIUM SERIES

ADSORPTION

96 Developments in Physical Adsorption
117 Adsorption Technology

219 Recent Advances in Adsorption and Ion Exchange

230 Adsorption and Ion Exchange—'83
233 Adsorption and Ion Exchange—Progress and Future Prospects

AEROSPACE

33 Rocket and Missile Technology

52 Chemical Engineering Techniques in Aerospace

BIOENGINEERING

69 Bioengineering and Food Processing
84 The Artificial Kidney
86 Bioengineering ... Food
93 Engineering of Unconventional Protein Production

99 Mass Transfer in Biological Systems
108 Food and Bioengineering—Fundamental and Industrial Aspects
114 Advances in Bioengineering
163 Water Removal Processes: Drying and Concentration of Foods and Other Materials

172 Food, pharmaceutical and bioengineering—1976/77
181 Biochemical Engineering Renewable Sources of Energy and Chemical Feedstocks

CRYSTALLIZATION

110 Factors Influencing Size Distribution
193 Design Control and Analysis of Crystallization Processes

215 Nucleation, Growth and Impurity Effects in Crystallization Process Engineering

240 Advances in Crystallization From Solutions

DRAG REDUCTION

111 Drag Reduction

130 Drag Reduction in Polymer Solutions

ENERGY

Conversion and Transfer

5 Heat Transfer, Atlantic City
57 Heat Transfer, Boston
59 Heat Transfer, Cleveland
75 Energy Conversion Systems
79 Heat Transfer with Phase Change
87 Advances in Cryogenic Heat Transfer

113 Convective and Interfacial Heat Transfer
118 Heat Transfer—Tulsa
119 Commercial Power Generation
138 Heat Transfer—Research and Design
162 Energy and Resource Recovery from Industrial and Municipal Solid Wastes

174 Heat Transfer: Research and Application
189 Heat Transfer—San Diego 1979
202 Transport with Chemical Reactions
208 Heat Transfer—Milwaukee 1981
216 Processing of Energy and Metallic Minerals
225 Heat Transfer—Seattle 1983
236 Heat Transfer—Niagara Falls 1984

Nuclear Engineering

53 Part XIII
56 Part XIV
94 Part XX
104 Part XXI

106 Part XXII
119 Commercial Power Generation
168 Heat Transfer in Thermonuclear Power Systems

169 Developments in Uranium Enrichment
191 Nuclear Engineering Questions Power Reprocessing, Waste, Decontamination Fusion
221 Recent Developments in Uranium Enrichment

ENVIRONMENT

78 Water Reuse
97 Water—1969
115 Important Chemical Reactions in Air Pollution Control
122 Chemical Engineering Applications of Solid Waste Treatment
124 Water—1971
126 Air Pollution and its Control
133 Forest Products and the Environment
137 Recent Advances in Air Pollution Control
139 Advances In Processing and Utilization of Forest Products
144 Water—1974: I. Industrial Wastewater Treatment
145 Water—1974: II. Municipal Wastewater Treatment
146 Forest Product Residuals
147 Air: I. Pollution Control and Clean Energy
148 Air: II. Control of NO_{xx} and SO_x Emissions
149 Trace Contaminants in the Environment
151 Water—1975
156 Air Pollution Control and Clean Energy

157 New Horizons for the Chemical Engineer in Pulp and Paper Technology

165 Dispersion and Control of Atmospheric Emissions, New-Energy-Source Pollution Potential
170 Intermaterials Competition in the Management of Shrinking Resources
171 What the Filterman Needs to Know About Filtration
175 Control and Dispersion of Air Pollutants: Emphasis on NO_x and Particulate Emissions
177 Energy and Environmental Concerns in the Forest Products Industry
184 Advances in the Utilization and Processing of Forest Products
188 Control of Emissions from Stationary Combustion Sources Pollutant Detection and Behavior in the Atmosphere
195 The Role of Chemical Engineering in Utilizing the Nation's Forest Resources
196 Implications of the Clean Air Amendments of 1977 and of Energy Considerations for Air Pollution Control

198 Fundamentals and Applications of Solar Energy

200 New Process Alternatives in the Forest Products Industries
201 Emission Control from Stationary Power Sources: Technical, Economic and Environmental Assessments
207 The Use and Processing of Renewable Resources—Chemical Engineering Challenge of the Future
209 Water—1980
210 Fundamentals and Applications of Solar Energy II
211 Research Trends in Air Pollution Control: Scrubbing, Hot Gas Clean-up, Sampling and Analysis
213 Three Mile Island Cleanup
223 Advances in Production of Forest Products
232 Applications of Chemical Engineering in the Forest Products Industry
239 The Impact of Energy and Environmental Concerns on Chemical Engineering in the Forest Products Industry

FLUIDIZATION

101 Fundamental Processes in Fluidized Beds
105 Fluidization Fundamentals and Application
116 Fluidization: Fundamental Studies Solid-Fluid Reactions, and Applications

176 Fluidization Application to Coal Conversion Processes
205 Recent Advances in Fluidization and Fluid-Particle Systems

234 Fluidization and Fluid Particle Systems: Theories and Applications
241 Fluidization and Fluid Particle Systems: Recent Advances

HISTORY OF CHEMICAL ENGINEERING

The History of Penicillin Production

235 Diamond Jubilee Historical/Review Volume

ION EXCHANGE

Adsorption and Ion Exchange Separations
Recent Advances in Adsorption and Ion Exchange

230 Adsorption and Ion Exchange—'83

233 Adsorption and Ion Exchange—Progress and Future Prospects

KINETICS

Reaction Kinetics and Unit Operations

73 Kinetics and Catalysis

MATHEMATICS

MINERALS

Mineral Engineering Techniques
Fossil Hydrocarbon and Mineral Processing

173 Fundamental Aspects of Hydrometallurgical Processes

180 Spinning Wire from Molten Metals
216 Processing of Energy and Metallic Minerals

PETROCHEMICALS

Polymer Processing
Declining Domestic Reserves—Effect on Petroleum and Petrochemical Industry

135 The Petroleum/Petrochemical Industry and the Ecological Challenge

142 Optimum Use of World Petroleum
212 Interfacial Phenomena in Enhanced Oil Recovery

PETROLEUM PROCESSING

C_4 Hydrocarbon Production and Distribution
Declining Domestic Reserves—Effect on Petroleum and Petrochemical Industry

135 The Petroleum/Petrochemical Industry and the Ecological Challenge
142 Optimum Use of World Petroleum

155 Oil Shale and Tar Sands
226 Underground Coal Gasification: The State of the Art

PHASE EQUILIBRIA

Pittsburgh and Houston

6 Collected Research Papers

88 Phase Equilibria and Gas Mixtures Properties

PROCESS DYNAMICS

Process Dynamics and Control
Process Systems Engineering

55 Process Control and Applied Mathematics

214 Selected Topics on Computer-Aided Process Design and Analysis

SEPARATION

Recent Advances in Separation Techniques

192 Recent Advances in Separation Techniques—II

SONICS

109 Sonochemical Engineering

THERMODYNAMICS

TRANSPORT PROPERTIES

56 Selected Topics in Transport Phenomena

MISCELLANEOUS

Chemical Engineering Reviews
Small-Scale Equipment for Chemical Engineering Laboratories
Engineering, Chemistry, and Use of Plasma Reactors
Vacuum Technology at Low Temperatures
Standardization of Catalyst Test Methods
Biorheology
The Modern Undergradate Laboratory Innovative Techniques

186 Plasma Chemical Processing
187 Chronic Replacement of Kidney Function
194 Hazardous Chemical—Spills and Waterborne Transportation
203 A Review of AIChE's Design Institute for Physical Property Data (DIPPR) and Worldwide Affiliated Activities
204 Tutorial Lectures in Electrochemical Engineering and Technology
206 Controlled Release Systems

217 New Composite Materials and Technology
220 Uncertainty Analysis for Engineers
228 Problem Solving
229 Tutorial Lectures in Electrochemical Engineering and Technology—II
231 Data Base Implementation and Application
237 Awareness of Information Sources
238 New Developments in Liquid-Liquid Extractors: Selected Papers From ISEC '83

Electro Organic Synthesis Technology

MONOGRAPH SERIES

The Manufacture of Nitric Acid by the Oxidation of Ammonia—The DuPont Pressure Process by Thomas H. Chilton
Experiences and Experiments with Process Dynamics by Joel O. Hougen
Present Past, and Future Property Estimation Techniques by Robert C. Reid

6 Catalysts and Reactors by James Wei
7 The 'Calculated' Loss-of-Coolant Accident by L.J. Ybarrondo, C.W. Solbrig, H.S. Isbin
8 Understanding and Conceiving Chemical Process by C. Judson King
9 Ecosystem Technology: Theory and Practice by Aaron J. Teller

10 Fundamentals of Fire and Explosion by Daniel R. Stull
11 Lumps, Models and Kinetics in Practice by Vern W. Weekman, Jr.
12 Lectures in Atmospheric Chemistry by John H. Seinfeld
13 Advanced Process Engineering by James R. Fair
14 Synfuels from Coal by Bernard S. Lee

CONTENTS

FOREWORD III

CHARACTERISTICS OF ERUPTING BUBBLES IN A THREE DIMENSIONAL FLUIDIZED BED ..... Edward K. Levy, Ismail Alkan, Hugo Karam 1

RADIAL DISTRIBUTION OF BUBBLES IN THE CYLINDRICAL FLUIDIZED BED ..... S. Mori, S. Miho, S. Hiraoka, I. Yamada 10

GAS DISTRIBUTION AND HEAT TRANSFER IN A DRAFT-TUBE SPOUTED BED ..... J.K. Claflin, A.G. Fane 17

THE EFFECT OF SYSTEM PRESSURE ON THE TRANSPORT DISENGAGING (TDH) ABOVE BUBBLING GAS-FLUIDIZED BEDS ..... I.H. Chan, T.M. Knowlton 24

PRESSURE DROP ACROSS THE DISTRIBUTOR IN FLUIDIZED BEDS WITH REGULAR AND AND IRREGULAR DISTRIBUTOR DESIGN ..... Tho-Ching Ho, T.K. Chen, J.R. Hopper 34

DISTRIBUTOR ZONE REACTION IN A GAS-FLUIDIZED BED ..... Yang Xiao-tian, D.G. Horne, J.G. Yates, P.N. Rowe 41

THE MECHANICS OF PARTICLE MOTION IN A GRID JET ..... B. Patrose, H.S. Caram 48

HYDRONAMICS OF FLUIDIZATION: BUBBLES AND GAS COMPOSITIONS IN THE U-GAS PROCESS ..... Dimitri Gidaspou, Bozorg Ettediah, Jacques Bouillard 57

FLUIDIZED BED REACTOR MODELLING ..... Q.M. Mao, O.E. Potter 65

EXPLORATIONS INTO THERMODYNAMIC ANALOGIES AND CRITICAL POINTS IN REFERENCE TO GAS-SOLID TRANSPORT ..... Mahendra P. Mathur, David J. Wildman, S. T. Tuba, G.E. Klinzing 72

EFFECT OF TEMPERATURE ON THE DENSE PHASE IN HIGH PRESSURE FLUIDIZED BEDS OF FINE POWDERS ..... Alan W. Weimer, George J. Quarderer 79

PRELIMINARY STUDY OF A RADIANTLY HEATED FLUIDIZED BED FOR THE PRODUCTION OF HIGH-PURITY SILICON ..... Octave Levenspiel, Milton B. Larson, Guo-Tai Zhang, Fan Ouyang 87

GAS FLUIDIZATION OF SOLIDS IN A STATIONARY LIQUID ... J.D. Gabor, J.C. Cassulo, D. Fountain, J.D. Bingle 95

SOME REMARKS ON GAS-LIQUID MASS TRANSFER AND BIOLOGICAL PHENOL DEGRADATION IN A DRAFT TUBE GAS-LIQUID-SOLID FLUIDIZED BED BIOREACTOR..... Liang-Shih Fan, K. Fujie, T.R. Long 102

BUBBLE PHENOMENA IN THREE-PHASE FLUIDIZED BEDS AS VIEWED BY A U-SHAPED FIBER OPTIC PROBE ..... S.L.P. Lee, H.I. de Lasa, M.A. Bergougnou 110

RADIAL SOLID DENSITY VARIATION IN A FAST FLUIDIZED BED ..... H. Weinstein, M. Shao, L. Wasserzug 117

MEASUREMENT METHOD OF FLOW VELOCITY OF LIQUID AND IRREGULAR SOLID PARTICLES USING AN IMAGE SENSOR WITH AN IMAGE FIBER ..... Mitsou Kamiwano, Fumio Saito 122

CROSSFLOW MAGNETICALLY STABILIZED FLUIDIZED BEDS .....J.H. Siegell, C.A. Coulaloglou 129

IN SITU OBSERVATION OF AEROSOL FILTRATION IN A TWO-DIMENSIONAL MODEL FILTER..... K. Ushiki, Chi Tien 137

INCLINED FLUIDIZED BED ..... Y.O. Chong, Thu-Hang Nguyen, L.S. Leung, C.S. Teo 149

HEAT TRANSFER BETWEEN MOVING BED OF SOLIDS AND IMMERSED CYLINDERS ..... M. Colakyan, O. Levenspiel 156

THE INFLUENCE OF BAFFLE DESIGN ON FLUIDIZATION CHARACTERISTICS IN A FLUID BED UNIT SYSTEM..... H.O. Kono, M. Jinnai 169

THREE-PHASE FLUIDIZATION OF POLYDISPERSE BEADS .....V.T. Sinha, M. Butensky, D. Hyman 176

CHARACTERISTICS OF ERUPTING BUBBLES IN A THREE DIMENSIONAL FLUIDIZED BED

E.K. Levy, I. Alkan and H. Caram ■ Lehigh University, Bethlehem, Pennsylvania

Measurements were made of the bubbling processes at the free surface of a three dimensional fluidized bed to determine the effects of operating conditions on the characteristics of the erupting bubbles; and calculations were carried out to determine the magnitude of the bubble through-flow coefficient and effective area of flow. The results show that the bubble through-flow coefficient is much larger than is predicted by classical bubble models, ranging from two to eight for glass particles and fourteen to nineteen for puffed millet bed material. The percentage of coalescing bubbles increased with superficial gas velocity to values approaching 25 percent. Horizontal coalescence between bubbles was found to have a negligible effect on the height to which the bulge and wake materials are ejected during an eruption process.

SCOPE

As bubbles erupt from the surface of a gas fluidized bed, particles are projected upwards into the freeboard. Some are subsequently carried from the bed by their initial momentum and the gas motion, while others fall back onto the bed surface. In developing a mechanistic model to relate the basic characteristics of the fluidized bed to elutriation rate, it is necessary to have information on quantities such as the size of the erupting bubbles, the frequency with which they erupt and the gas velocities within the bubble and in the surrounding region. Theories are available on the absolute rise velocity of a bubble as a function of size, superficial gas velocity and minimum fluidization velocity and correlations have been developed to predict the size of a bubble as a function of fluidization conditions. In addition, the two-phase theory of fluidization is commonly used to relate bubble fraction and bubble frequency to other bubbling parameters.

In the existing study, measurements of the bubbling processes at the free surface of a three dimensional bed were made using 264 micron glass beads and 4304 micron puffed millet particles to determine the effects of bed depth and fluidizing velocity on the eruption frequency, size and area fraction occupied by the erupting bubbles. Calculations were then carried out using existing bubble growth correlations, bubble velocity models and a modified two-phase theory of fluidization to attempt to predict the measured eruption frequencies and bubble fractions on a theoretical basis and to determine the magnitudes of the bubble through-flow coefficient and effective area of flow.

Experiments were also performed where the relative importance of individual bubbles and bubbles which coalesce vertically during eruption was measured. In addition, the effect of horizontal interactions between adjacent bubbles at the free surface of the bed was studied.

CONCLUSIONS AND SIGNIFICANCE

From measurements of the erupting bubbles at the free surface, relationships were obtained between the maximum frontal diameter, D_i, and the equivalent diameter, D_e, where with the glass beads $D_i/D_e = 1.154$ and for the larger puffed millet particles $D_i/D_e = 1.254$. The data on bubble size as a function of bed depth and fluidizing velocity were compared to three bubble growth correlations and were found to be in very good agreement with the correlation due to Kato and Wen. Data on the absolute rise velocity of the bubbles as they reach the free surface were obtained for both kinds of particles and were found to agree with the standard expression for bubble rise velocity.

Equations, based on a modified form of the two-phase theory of fluidization were derived which account for variations in both the through flow coefficient m and on the equivalent diameter for bubble gas flow across the horizontal plane at the surface of the bed. Using measured data for bubble eruption frequency and for the number of bubbles at the free surface, the experimental data were used to compute the values of ϕ_f and m. The results show that the through-flow coefficient m is much larger than is predicted by the Davidson bubble analysis, being in the range of 2 to 8 for the glass particles and 14 to 19 for puffed millet. In both cases the effective flow diameter D_f, is smaller than the equivalent spherical diameter, D_e, with values of ϕ_f = 0.6 for millet and 0.85 to 1.0 for glass.

It is physically reasonable to expect relatively high values of m at the free surface of the bed, because of the nature of the boundary conditions exerted on the gas flow in the vicinity of the bubble as the bubble approaches the free surface. However, additional work is needed in analyzing this situation and in obtaining direct experimental confirmation of the values of m. In addition, careful experimental measurements are needed to obtain more reliable information on the velocity of the gas in the emulsion phase.

Data were obtained on the proportion of the bubbles erupting at the free surface which were individual isolated bubbles and the fraction which were bubbles in the process of undergoing vertical coalescence. It was found that the percentage of double bubbles increased with superficial gas velocity to values approaching 25 percent. Data were analyzed on bubbles undergoing horizontal coalescence; and this was found to have negligible effect on the height to which the bulge and wake materials are ejected during an eruption process.

THEORETICAL DEVELOPMENT

The original two-phase theory of fluidization developed by Toomey and Johnstone (1), proposed that all the gas flow in excess of the minimum needed to fluidize the emulsion phase passes through the bed in the form of bubbles. The resulting theoretical visible bubble flow rate consistently overpredicts actual measurements; and the difference between the two is generally attributed to either one of two factors:

- Some investigators, (2 to 5) relate the failure of the basic two-phase theory to an increase in dense phase gas velocity to values in excess of U_{mf}. On the other hand, Geldart (6) argues that U_e is approximately equal to U_{mf}.
- Other investigators have argued that the failure of the basic two-phase theory is due primarily to gas flow within the bubble. This leads to a modified form of the two-phase theory, where the gas inside a rising bubble has a mean velocity mU_{mf} relative to the bubble.

  Modeling the flow of the emulsion phase around a bubble void as an incompressible irrotational fluid and calculating the gas flow field relative to the moving bubble from Darcy's law, Davidson (7) derived expressions for the flow of gas through the bubble and found that m = 0 for fast bubbles and three for slow bubbles. When Davidson's values for m are used with the two-phase theory modified to account for the presence of gas through-flow, the theory still predicts visible bubble flow rates which are much higher than those measured. Based on measurements of erupting bubbles as seen from the top of the bed, point frequency measurements, bed expansion measurements and other types of data, numerous investigators (for example, 5, 8, 9, 10) have reported values of m far in excess of three. Reasons for the discrepancy have been attributed to bubble-bubble interactions, bubble wall interactions and the effect of bubble shape on through flow (9 to 13).

Because of the need in the present work to develop a procedure for accurately predicting bubble eruption frequency and bubble size as functions of the operating properties of the bed, a careful review of bubble theory was undertaken. A derivation of the mass conservation equations in terms of variables important to this work is described in the following.

Assuming the gas flow is steady and incompressible and applying the conservation of mass principle to the surface of the bed gives

$$U_o A_o = (\delta V_{GI} + (1 - \delta) U_e) A_o \quad (1)$$

The absolute velocity of the gas flowing through the bubble V_{GI} can be expressed as

$$V_{GI} = U_b + mU^* \quad (2)$$

Combining (1) and (2) to obtain the fraction of the surface area occupied by bubbles

$$\delta = \frac{U_o - U_e}{U_b + mU^* - U_e} \quad (3)$$

If the gas flow area provided by each erupting bubble is $\pi D_f^2/4$, the number of simultaneously erupting bubbles is

$$N = \frac{\delta A_o}{\frac{\pi}{4}(\phi_f D_e)^2}$$

or

$$N = \frac{(U_o - U_e)\, 4A_o}{\pi \phi_f^2 D_e^2 [U_b + mU^* - U_e]} \quad (4)$$

where the quantity D_f can be related to the equivalent bubble diameter D_e through

$$\phi_f = D_f/D_e \quad (5)$$

The fraction of the surface occupied by bubbles is also related to the visible bubble flow rate

$$\delta A_o U_b = \dot{n} V_{bubble} \quad (6)$$

This can be combined with Equation (3) to give the bubble frequency

$$\dot{n} = \frac{(U_o - U_e) A_o U_b}{(U_b + mU^* - U_e) \frac{\pi}{6} D_e^3} \quad (7)$$

Both the values of $\dot{n}$ and N can be measured experimentally and Equations (4) and (7) can be used to determine the values of the shape factor ϕ_f and the through flow coefficient m if the values for U_e, U_b, and D_e are provided by experiments or correlations.

The absolute bubble velocity U_b is usually computed from the relation

$$U_b = U_o - U^* + 0.711 \sqrt{gD_e} \quad (8)$$

while the equivalent bubble diameter can be obtained from the Kato & Wen (13) correlation

$$D_e = 1.4\, d_p \rho_p \frac{U_o}{U_{mf}} L + D_{eo} \quad (9)$$

This requires the initial bubble diameter D_{eo} correlated by Chiba et al (14)

$$D_{eo} = 0.347 [A_o (U_o - U_{mf})/N_o]^{0.4} \quad (10)$$

Assuming the bed expansion is due to the existence of bubbles, the bed height L is obtained from the relation

$$\frac{L - L_{mf}}{L} = \frac{U_o - U_e}{U_b + mU^* - U_e} \quad (11)$$

EXPERIMENTAL APPARATUS AND PROCEDURE

All of the experiments described in this paper were performed in a 76 x 76 cm square bed. The front wall was made of plexiglass to permit visualization of bubble surface eruptions. The distributor was a steel plate drilled with 484 holes (0.4 cm diameter). Room temperature air at atmospheric pressure was supplied to the bed from a laboratory compressor. Air flow rate to the bed was measured using orifice meters designed according to ASME specifications.

All the bubble eruption measurements were made using a Videologic Co. INSTAR high speed video system. This system is capable of recording and playing at a rate of 120 frames per second and has a slow motion feature which allows the user to observe the film frame by frame. The dual cameras make it possible to take pictures of two different parts of the bed at the same time and display these simultaneously on a split screen. Most of the experiments were performed using both video cameras, one focusing on the bed surface through a tilted mirror located above the bed, the other looking directly through the front wall of the bed.

All experiments were performed in a freely bubbling mode. At each bed height, different flow rates were recorded until the flow rate was so high that the eruptions became chaotic and effective flow visualization became difficult. Each run was played back in slow motion and the number of bubbles at the free surface, bubble frequency, bubble eruption diameters, bulge and wake ejection heights, fraction of double bubbles and the nature of horizontal coalescences were recorded for each set of conditions.

The bubble count N (number of bubbles at the free surface at a given instant of time) was analyzed using recordings taken from above the bed. Only bubbles through which gas was flowing were included in this quantity. These are referred to here as "active" bubbles and were characterized by the upward motion of the bulge material. Bubbles were included in N if their bulges were rising in consecutive video frames. When the wake of a bubble was first observed, the bubble was no longer considered active and at that point was no longer counted as being part of N. Bubble eruption frequency ($\dot{n}/A_0$) was measured from the same film sequences, where the rate of surface eruptions was counted with the film advancing in slow motion.

The bubble eruption diameters, D_j were measured from the front wall of the bed, where the largest width of the observed bubble is defined here as the eruption diameter (Figure 1). At least 100 bubbles were counted at each bed height and flow rate and the arithmetic average of the diameters of the bubbles was computed.

Two different types of particles were used in the experiments: glass beads with a mean diameter of 264 microns and 4304 micron puffed millet particles. Both fall into the range of group B particles according to Geldart's classification (15). The glass beads have a density of 2.50 g/cm^3 and the density for the puffed millet particles was 0.131 g/cm^3. The sphericity of the millet particles was 0.766.

The minimum fluidization velocity for the glass particles was calculated to be 5.68 cm/s, with a measured value of 5.97 cm/s. In the case of the puffed millet, even though the bed appeared to fluidize normally, the pressure drop-flow rate characteristics were unusual in that the bed pressure drop continued to increase beyond the minimum fluidization point. Minimum fluidization was observed to occur at a velocity of 11.6 cm/s; and the minimum bubbling velocity was found to be 17.6 cm/s.

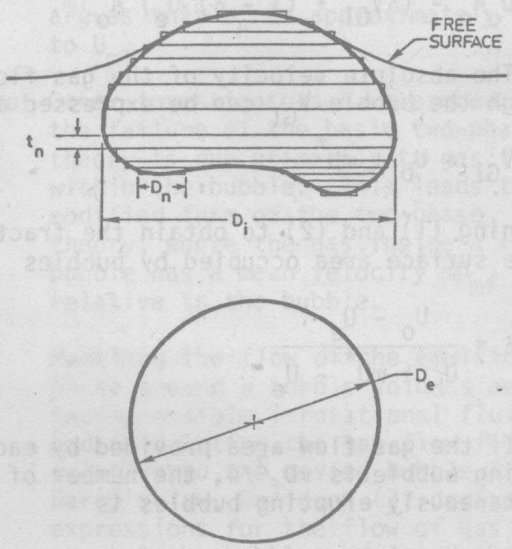

Figure 1. Sketch of bubble at free surface illustrating definitions of frontal diameter, D_j, and equivalent spherical diameter. D_e.

RESULTS

Separate experiments were carried out with both the small glass beads and the puffed millet particles over a range of bed depths and superficial gas velocities, where video sequences were taken of the bubbling behavior at the side and top of the bed at the free surface. There are three characteristic diameters of importance in this study.

- D_f, the effective diameter of the circular eruption areas through which gas flows vertically across the free surface of the bed
- D_j, the frontal bubble diameter measured at the sidewall as shown in Figure 1
- D_e, the equivalent bubble diameter defined as the diameter of a sphere having the same volume as the actual bubble.

Almost all of the bubble growth correlations are expressed in terms of the equivalent bubble diameter, D_e, but this is a quantity

which cannot be measured directly. As an alternative, D_i, was obtained from the video sequences. With the assumption that the bed sidewall cuts the bubbles into equal halves, photographs of the bubble cross sections were taken. These were divided into small elemental areas and the individual volumes of the resulting discs of revolution were computed and added together to determine total bubble volume. This then was set equal to the volume of a sphere of equivalent diameter D_e and the bubble shape factor $\phi_i = D_i/D_e$ was evaluated (see Figure 1). The results show average values of ϕ_i of 1.154 for the glass particles and 1.254 for the puffed millet. Bubble shape seems to depend slightly on superficial gas velocity and bed depth, but the average values given above were found to work well in subsequent analyses.

The measured values of D_i, converted to D_e, were compared to three different bubble growth models (13, 16, and 17). It was found that the Kato and Wen model (13) gave the best results, agreeing well with the measurements for both the small and large particles (see Figure 2).

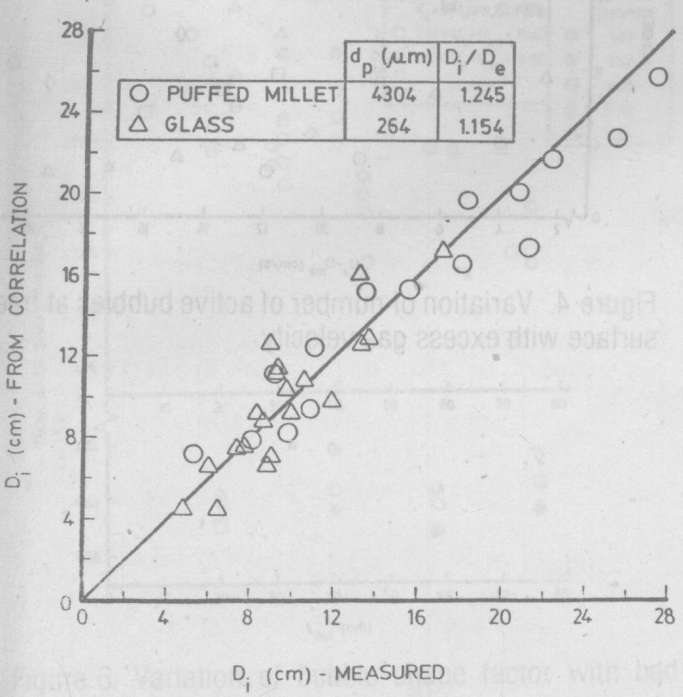

Figure 2. Comparison of measured bubble eruption diameters with the Kato & Wen bubble growth correlation.

Absolute bubble rise velocities were measured by obtaining the relationship between the vertical position of a given bubble and time from the video sequences. The resulting velocity at the instant that the top of the bubble crosses the undisturbed free surface of the bed was interpreted as the absolute bubble rise velocity at the free surface. This velocity is plotted in Figure 3 as $(U_b - (U_o - U_{mf}))$ in the case of the glass particles and $(U_b - (U_o - U_{mb}))$ in the case of the puffed millet. These results, obtained for bubbles over a range of conditions, show that Equation 8, the standard equation for bubble rise velocity, agrees with measurements at the free surface. Similar conclusions were reached by Levy et al (18) with styrene particles and glass beads.

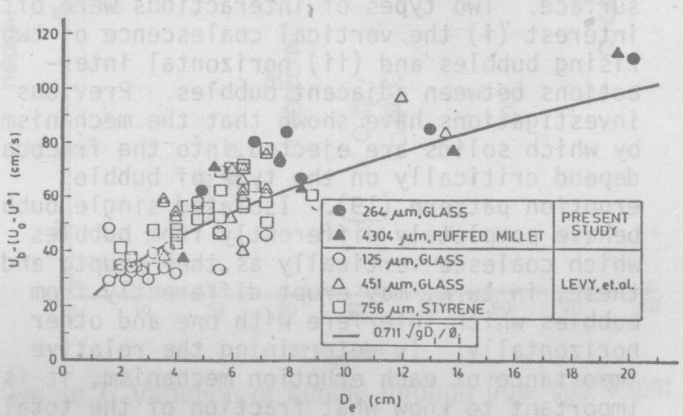

Figure 3. Absolute bubble rise velocity at free surface of bed.

Data on the number of active bubbles N and the frequency of bubble eruptions (n/A) were obtained from video sequences taken of the bed surface from the freeboard. The results for glass, summarized in Figures 4 and 5 show that N and n/A are both decreasing functions of bed height and excess flow velocity. Similar results were obtained for the puffed millet.

Equations 4 and 7 provide two theoretical relationships for N and n/A in terms of the parameters U_e, m, ϕ_f, D_e and U_b. The bubble rise velocity U_b was computed from Equation 8, the equivalent diameter was found from the Kato and Wen correlation; and the gas velocity in the emulsion phase U_e was assumed equal to U_{mf} for the glass beads and

U_{mb} for the millet. Using the measured values for N and $\dot{n}/A$, Equations 4 and 7 were then solved simultaneously for m and ϕ_f, the results of which are shown in Figures 6 and 7. In the case of the millet, $\phi_f = 0.6$ and is relatively independent of both bed depth and superficial gas velocity. On the other hand with the glass particles, ϕ_f ranges from 0.85 to 1 and is a strong function of bed depth. The through-flow coefficient m appears to depend primarily on bed depth, ranging from two to values exceeding eight with glass. In the case of the puffed millet, m ranged from 14 to 19.

As part of this effort, data were obtained on the nature of the interactions between bubbles as they erupt from the free surface. Two types of interactions were of interest (i) the vertical coalescence of two rising bubbles and (ii) horizontal interactions between adjacent bubbles. Previous investigations have shown that the mechanisms by which solids are ejected into the freeboard depend critically on the type of bubble eruption pattern (19). Isolated single bubbles behave completely differently from bubbles which coalesce vertically as they erupt; and these, in turn, may erupt differently from bubbles which interfere with one and other horizontally. In determining the relative importance of each eruption mechanism, it is important to know what fraction of the total number of bubble eruptions is of each type. Figure 8 is the fraction of the total bubble eruptions which occur as vertical coalescences (double bubbles) for the 264 micron glass beads. The percentage of double bubbles is a strong function of the superficial gas velocity and bed depth, increasing to values above 20 percent.

As a single bubble erupts from the free surface, material at the nose of the bubble is carried upward to a certain height before falling back toward the bed surface. This, in turn, is followed by the wake material which typically rises to a smaller vertical height than the bulge. Data on the nature of these eruptions for the glass bead material were obtained by observing a large number of bubbles. The results show that the dimensionless heights reached by the bulge and wake increase very slightly with both bed depth and gas velocity. Mean values are

$$(H/D_i)_{max} = 0.75 \text{ for the bulge}$$

$$(H/D_i)_{max} = 0.48 \text{ for the wake}$$

Levy et al (18) previously reported the values

$$(H/D_i)_{max} = 0.6 \text{ for the bulge}$$

$$(H/D_i)_{max} = 0.33 \text{ for the wake}$$

and the differences may be due to differences in the sizes of the beds employed in the two experiments.

Similar analyses for two bubbles erupting side by side, show that the dimensionless heights to which the bulge and wake materials are ejected are the same as for isolated bubbles. Horizontal coalescence appears to have no effect on the heights to which the bulge and wake materials are projected.

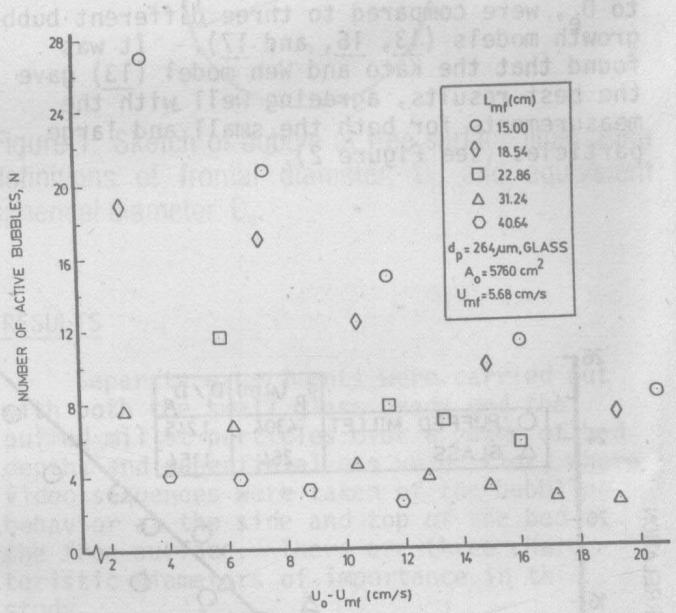

Figure 4. Variation of number of active bubbles at free surface with excess gas velocity.

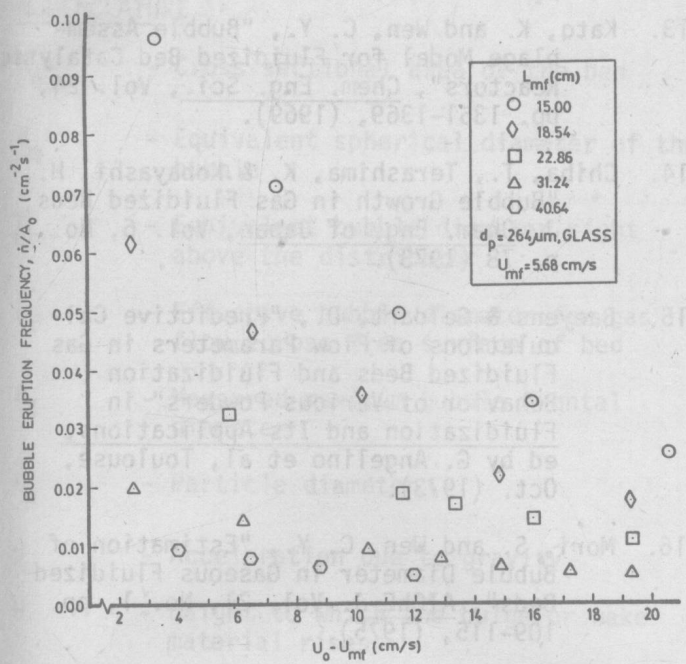

Figure 5. Variation of bubble eruption frequency with excess gas velocity.

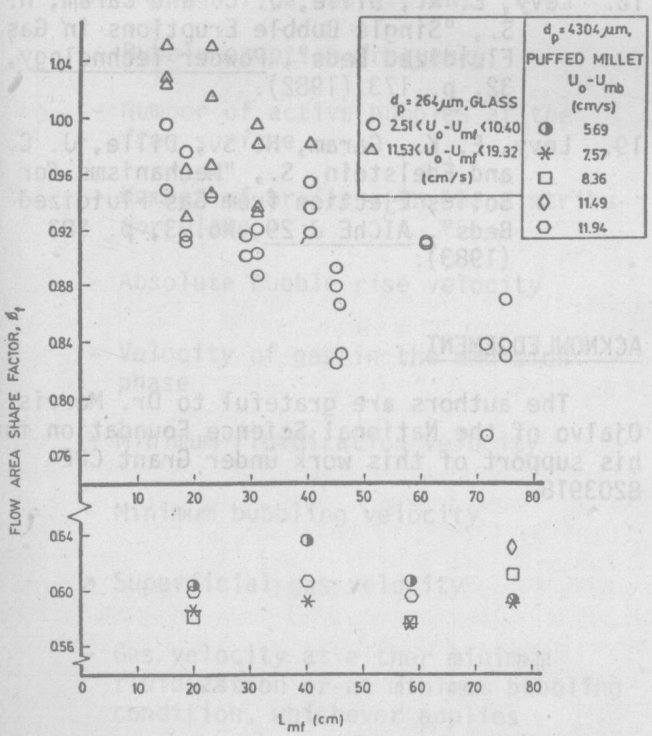

Figure 6. Variation of bubble shape factor with bed depth.

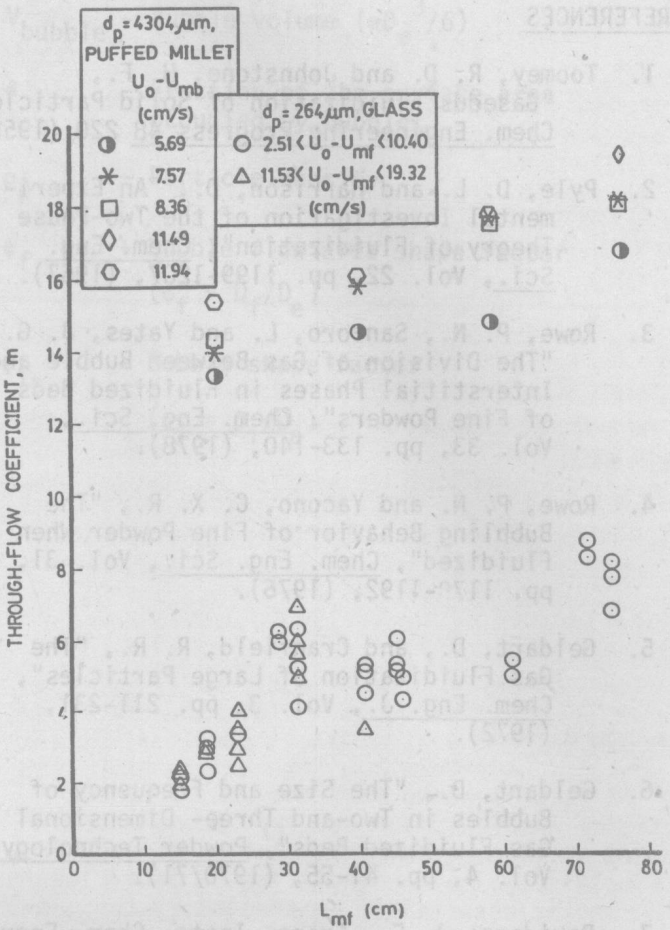

Figure 7. Variation of bubble through flow coefficient with bed depth.

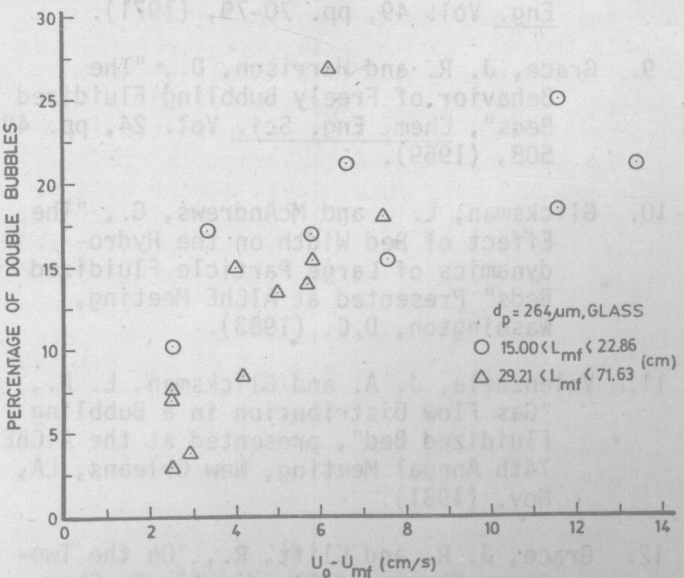

Figure 8. Variation of percentage of double bubbles with excess gas velocity.

REFERENCES

1. Toomey, R. D. and Johnstone, H. F., "Gaseous Fluidization of Solid Particles" Chem. Engineering Progress 48 220 (1952).

2. Pyle, D. L. and Harrison, D., "An Experimental Investigation of the Two-Phase Theory of Fluidization", Chem. Eng. Sci., Vol. 22, pp. 1199-1207, (1967).

3. Rowe, P. N., Santoro, L. and Yates, J. G., "The Division of Gas Between Bubble and Interstitial Phases in Fluidized Beds of Fine Powders", Chem. Eng. Sci., Vol. 33, pp. 133-140, (1978).

4. Rowe, P. N. and Yacono, C. X. R., "The Bubbling Behavior of Fine Powder When Fluidized", Chem. Eng. Sci., Vol. 31, pp. 1179-1192, (1976).

5. Geldart, D., and Cranfield, R. R., "The Gas Fluidization of Large Particles", Chem. Eng. J., Vol. 3, pp. 211-231, (1972).

6. Geldart, D., "The Size and Frequency of Bubbles in Two-and Three- Dimensional Gas Fluidized Beds", Powder Technology, Vol. 4, pp. 41-55, (1970/71).

7. Davidson, J. F., Trans. Instn. Chem. Engrs., 39, p. 230 (1961).

8. McGrath, L. and Streatfield, R. E., "Bubbling in Shallow Gas Fluidized Beds of Large Particles", Trans. Instn. Chem. Eng. Vol. 49, pp. 70-79, (1971).

9. Grace, J. R. and Harrison, D., "The Behavior of Freely Bubbling Fluidized Beds", Chem. Eng. Sci. Vol. 24, pp. 497-508, (1969).

10. Glicksman, L. . and McAndrews, G., "The Effect of Bed Width on the Hydrodynamics of Large Particle Fluidized Beds" Presented at AIChE Meeting, Washington, D.C. (1983).

11. Valenzuela, J. A. and Glicksman, L. R., "Gas Flow Distribution in a Bubbling Fluidized Bed", presented at the AiChE 74th Annual Meeting, New Orleans, LA, Nov. (1981).

12. Grace, J. R. and Clift, R., "On the Two-Phase Theory of Fluidization", Chem. Eng. Sci. Vol. 29, pp. 327-334, (1974).

13. Kato, K. and Wen, C. Y., "Bubble Assemblage Model for Fluidized Bed Catalytic Reactors", Chem. Eng. Sci., Vol. 24, pp. 1351-1369, (1969).

14. Chiba, T., Terashima, K. & Kobayashi, H., "Bubble Growth in Gas Fluidized Beds, J. Chem. Eng. of Japan, Vol. 6, No. 1, p. 78 (1973).

15. Baeyens & Geldart, D., "Predictive Calculations of Flow Parameters in Gas Fluidized Beds and Fluidization Behavior of Various Powders" in Fluidization and Its Applications, ed by G. Angelino et al, Toulouse, Oct. (1973).

16. Mori, S. and Wen, C. Y., "Estimation of Bubble Diameter in Gaseous Fluidized Beds", AIChE J. Vol. 21, No. 1, pp. 109-115, (1975).

17. Darton, R. C., LaNauze, R. D., Davidson, J. F., and Harrison, D., "Bubble Growth Due to Coalescence in Fluidized Beds", Trans. Instn. Chem. Eng., Vol. 55, pp. 274-280, (1977).

18. Levy, E. K., Dille, J. C. and Caram, H. S., "Single Bubble Eruptions in Gas Fluidized Beds", Powder Technology, 32, p. 173 (1982).

19. Levy, E. K., Caram, H. S., Dille, J. C. and Edelstein, S., "Mechanisms for Solids Ejection from Gas Fluidized Beds", AIChE J 29, No. 3, p. 383 (1983).

ACKNOWLEDGEMENT

The authors are grateful to Dr. Morris Ojalvo of the National Science Foundation for his support of this work under Grant CPE 8203918.

NOMENCLATURE

A_o - Cross sectional area of the bed

D_e - Equivalent spherical diameter of the bubble

D_{eo} - Equivalent bubble diameter right above the distributor

D_f - Effective bubble diameter for gas flow across free surface of bed

D_i - Measured maximum bubble frontal diameter

d_p - Particle diameter

g - Acceleration due to gravity

H - Height to which the bulge or wake material rises

L - Vertical distance above the distributor

L_{mf} - Bed height at minimum fluidization

m - Through flow coefficient

$\dot{n}$ - Bubble eruption frequency

N - Number of active bubbles at the free surface

N_o - Number of orifices in the distributor plate

U_b - Absolute bubble rise velocity

U_e - Velocity of gas in the emulsion phase

U_{mf} - Minimum fluidization velocity

U_{mb} - Minimum bubbling velocity

U_o - Superficial gas velocity

U^* - Gas velocity at either minimum fluidization or at minimum bubbling condition, whichever applies

V_{GI} - Absolute velocity of the gas flowing through the bubble

V_{bubble} - Bubble volume ($\pi D_e^3/6$)

δ - Fraction of the surface area occupied by bubbles

ρ_p - Particle density

ϕ_f - Bubble flow area shape factor ($\phi_f = D_f/D_e$)

ϕ_i - Bubble shape factor ($\phi_i = D_i/D_e$)